Electrically Switching Bistability of a Chiral Quasi-Homeotropic Liquid Crystal Device with Low Driving Voltage

2003 Jpn. J. Appl. Phys. 42 L1330

(http://iopscience.iop.org/1347-4065/42/11A/L1330)

Jpn. J. Appl. Phys. Vol. 42 (2003) pp. L 1330–L 1333
Part 2, No. 11A, 1 November 2003

Electrically Switching Bistability of a Chiral Quasi-Homeotropic Liquid Crystal Device with Low Driving Voltage

Chih-Yung HSIEH and Shu-Hsia CHEN*

Institute of Electro-Optical Engineering, National Chiao Tung University, 1001 Ta Hsueh Road, Hsinchu 300, Taiwan, Republic of China

(Received June 25, 2003; accepted September 8, 2003; published October 22, 2003)

We report a new electrically switching bistable chiral quasi-homeotropic liquid crystal device with low driving voltage. This device is operated from the initial twisted-homeotropic state to either $+90^\circ$ or -270° twisted static state showing dark and bright transmittances, respectively, using different switching processes. The critical applied voltage to achieve the switching bistability of our device is only 4.3 V, which is approximately twice its threshold voltage for Freedericksz transition. In addition, the switching characteristics of this device with different driving waveforms are also investigated in this paper. [DOI: 10.1143/JJAP.42.L1330]

KEYWORDS: liquid crystals, chiral, quasi-homeotropic, bistability

The bistable twisted nematic[1] (BTN) liquid crystal device, which can be electrically switched between two twisted configuration states, was first discovered by Berreman and Heffer in 1981. Afterward, several variations in the structure have been proposed, such as the traditional 2π-BTN,[1–5] π-BTN[6–9] and zenithal BTN devices.[10] Recently, our group has also demonstrated a bistable chiral quasi-homeotropic (BCQH) liquid crystal device,[11,12] whose directors on the top and bottom substrates are parallel. This device is operated from the initial homeotropic state to two different twisted configuration states by controlling the switching process. It uses liquid crystal (LC) material with negative dielectric anisotropy while the BTN device uses positive LCs. However, the high driving voltage of the BCQH cell, which is about six times its threshold voltage for Freedericksz transition, V_{th}, is a serious drawback. It involves high power consumption and limits the application of this device. To eliminate this problem, one can use a LC with high dielectric anisotropy to decrease the driving voltage. Unfortunately, commercial LCs with large negative dielectric anisotropy are rare.

In this paper, we present a new electrically switching bistable chiral quasi-homeotropic LC device with lower driving voltage than existing LC devices. Unlike the previous demonstrated BCQH device,[11,12] the field-off initial state of this device is the twisted-homeotropic state, whose directors on the substrates are twisted $+90^\circ$, and we name this new device the $\pi/2$ bistable chiral quasi-homeotropic ($\pi/2$-BCQH) device in this paper. It is operated from the field-off twisted-homeotropic state to two different field-on twisted static states with different switching processes. We have investigated the switching characteristics of this $\pi/2$-BCQH device with different driving waveforms. As a result, we obtained a low critical applied voltage of 4.3 V, which is about twice its V_{th} for the switching bistability of the $\pi/2$-BCQH cell by controlling the slew rate of the driving square pulses.

The operation principle of this $\pi/2$-BCQH device, which is similar to that of the BTN or the BCQH cell, is based on the mismatch of the intrinsic twist property of LCs and the boundary condition of directors imposed by the rubbing surfaces. In this device, the liquid crystal with a chiral dopant has a negative intrinsic pitch, whereas the boundary directors are considered to have a positive 90° twisted angle. Consequently, with the appropriate ratio of the cell gap to the intrinsic pitch (d/p), both $+90^\circ$ and -270° twisted states may have the same total free energy at the same applied voltage in some voltage region. By controlling the field-induced flow effect of directors, the initial twisted-homeotropic state can be switched into either the $+90^\circ$ or -270° twisted state. Experimentally, the sample was assembled with two indium-tin-oxide (ITO) glasses, which were coated with the polyimide JALS-2021 (JSR Co.) to form homeotropic alignment, and the cell gap was 7.2 μm. The LC material was ZLI-2806 (Merck Co.) which has negative dielectric anisotropy. We added about 0.5 wt% of S811 (Merck Co.) as a chiral dopant to obtain a suitable helix pitch length. The difference between the top and bottom azimuthal angles was determined to be $+90^\circ$ based on the rubbing direction on the substrates. The sample was placed between two crossed polarizers and driven by an arbitrary-waveform function generator. The rubbing direction of the bottom substrate was parallel or perpendicular to the transmissive axis of the front polarizer. A 1 mW He-Ne laser with a wavelength of 632.8 nm was used as the light source and the transient transmittance was detected by a photodiode.

Figure 1 indicates the measured transient transmittance of the $\pi/2$-BCQH cell with different driving waveforms whose amplitudes were 5 volts. Waveform A had a rapidly rising voltage and produced a strong fluid flow of LCs. However, Waveform B had a gradually rising slew rate ($dV/dt = 100\,\mathrm{V/s}$) which resulted in weak flow effects. Clearly, by controlling the flow effects of directors, the initial twisted-homoetropic ($\mathbf{H}_t$) state could be switched into two different twisted static states with different final transmittances, dark and bright. The bright twisted ($\mathbf{B}_t$) state was the $+90^\circ$ twisted state, which was similar to the field-on state of a conventional chiral homeotropic cell,[13–15] and the dark twisted ($\mathbf{D}_t$) state was the -270° twisted state, which was operated outside the region of Mauguin limitation and led to low transmittance. Both $\mathbf{B}_t$ and $\mathbf{D}_t$ states would return to the $\mathbf{H}_t$ state after turning off the external electric field. From our previous study,[12] we believe that the field-induced flow effect plays an important role in the switching bistability of our cell.

To illustrate the bistability of the cell and design more practical switching waveforms, we carried out three meas-

*E-mail address: shuhchen@mail.nctu.edu.tw

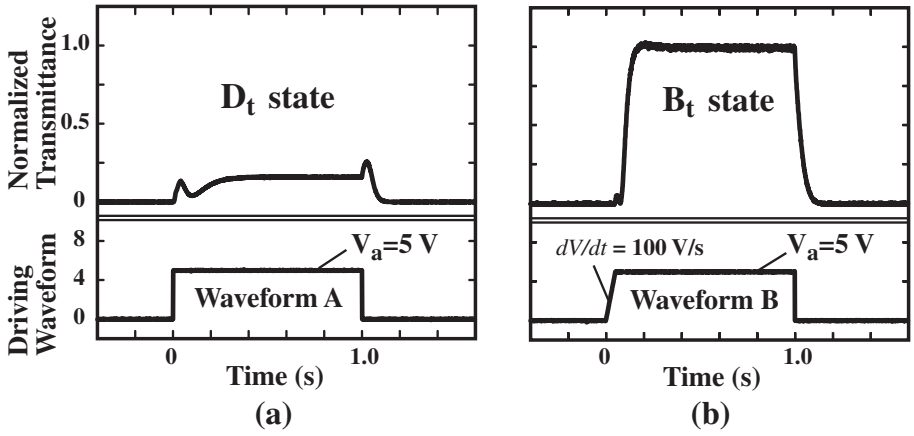

Fig. 1. Measured transient transmittance of our $\pi/2$-BCQH cell with different driving waveforms. The amplitudes of both waveforms A and B are 5 V. (a) The slew rate, dV/dt, of waveform A is infinite. (b) The slew rate, dV/dt, of waveform B is 100 V/s.

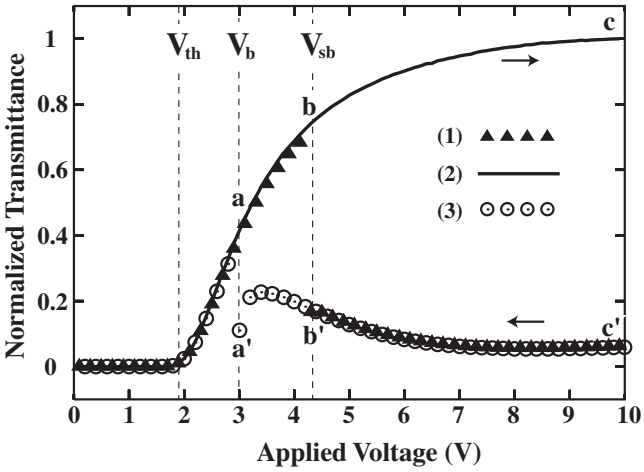

Fig. 2. Measured voltage-dependent static transmittance of our $\pi/2$-BCQH cell for different procedures. Curve (1) was the final transmittance of the cell applied with waveform A in Fig. 1, whose amplitude was increased from 0 to 10 V in steps of 0.1 V. A 1 kHz driving square wave was used for curves (2) and (3). The applied voltage, V_a, of curve (2) was increased from 0 to 10 V in steps of 0.1 V. The V_a of curve (3) was increased from 0 to 10 V abruptly in the beginning and then decreased gradually to 0 V in steps of 0.1 V.

urements with different voltage switching processes. The measured transmittance versus applied voltage plot is shown in Fig. 2. First, to determine the critical voltage to achieve the switching bistability of our $\pi/2$-BCQH cell, V_a, the amplitude of waveform A, shown in Fig. 1 was increased from 0 to 10 V in steps of 0.1 V. Note that the cell was switched from static $\mathbf{H_t}$ state at $V_a = 0$ V for every transmittance measurement. The transmittance of the static state is denoted as curve (1) in Fig. 2. There is an apparent discontinuous change in transmittance at the applied voltage $V_a = V_{sb} = 4.3$ V. Using a crossed-polarizer microscope, the optical texture was found to correspond to the states of $\mathbf{H}_t$, $\mathbf{B}_t$ and $\mathbf{D}_t$ under the Freedericksz threshold voltage V_{th}, between V_{th} and V_{sb} and above V_{sb}, respectively. However, when we applied waveform B with the same amplitude to the cell, it switched from the $\mathbf{H}_t$ state to the $\mathbf{B}_t$ state (not shown in Fig. 2). This result shows that V_{sb} is the critical voltage for the switching bistability of our $\pi/2$-BCQH cell obtained by controlling the slew rate of the driving square pulses shown in Fig. 1. It was only 4.3 V, which is smaller than that obtained in our previous BCQH cell.[11,12]

Next, the voltage-dependent behavior of the $\mathbf{B}_t$ state was studied. We applied a 1 kHz square wave to the cell and measured the static transmittance-voltage (TV) curve. The amplitude of the applied voltage, V_a, was increased in steps of 0.1 V from 0 to 10 V. Curve (2) in Fig. 2 shows the measured transmittance of the static state, which are $\mathbf{H}_t$ and $\mathbf{B}_t$ states under and above V_{th}, respectively. Finally, we applied abruptly a 10 V 1 kHz square wave to the cell so that the cell switched to the $\mathbf{D}_t$ state and then decreased gradually in steps of 0.1 V to 0 V. The results are denoted as curve (3) in Fig. 2. We found that, in addition to V_{th} and V_{sb}, there is another critical voltage, V_b, smaller than V_{sb}. Above V_b, the texture stays in the $\mathbf{D}_t$ state. Below V_b, it transits to the $\mathbf{B}_t$ state. Upon decreasing voltage to V_{th}, where it transits to the $\mathbf{H}_t$ state, it stays in the $\mathbf{B}_t$ state. The bistability behavior is described on the basis of measurements shown in Fig. 2 as follows.

Before V_{th}, the $\mathbf{H}_t$ state is the stable state. For $V_{th} < V_a < V_b$, the cell only exhibits the $\mathbf{B}_t$ state. Therefore, the cell does not have the bistable property in this region and V_b is the critical voltage of the bistability in our $\pi/2$-BCQH cell. In the region, $V_a \geq V_b$, the cell exhibits both the $\mathbf{B}_t$ and $\mathbf{D}_t$ states; therefore, the cell has the bistable property in this region. However, from the experiment for curve (1) in Fig. 2, we found that the field-induced flow effect by waveform A is insufficiently strong to switch the $\mathbf{H}_t$ state into the $\mathbf{D}_t$ state as $V_a < V_{sb}$. Moreover, the switching bistability in this region for $V_a < 4.3$ V is impossible to achieve using driving waveforms A and B in Fig. 1. Nevertheless, based on the information obtained from this phase diagram, since bistability exists between V_b and V_{sb}, one can reduce the holding voltage for the bistable states. Using a 1 kHz square-wave driving voltage, one can switch the cell from the $\mathbf{H}_t$ state to the $\mathbf{D}_t$ state with a selective voltage amplitude, V_s, larger than V_{sb} and then reduce the voltage to the desired holding voltage, V_h, between V_b and V_{sb} to maintain it in the $\mathbf{D}_t$ state. On the other hand, one can switch the cell from the $\mathbf{H}_t$ state to the $\mathbf{B}_t$ state and maintain it in the B_t state with a selective voltage, V_s, smaller than V_h. Therefore, with this procedure, we can achieve the switching bistability of the $\pi/2$-BCQH cell with any holding voltage larger than V_b instead of V_{sb}.

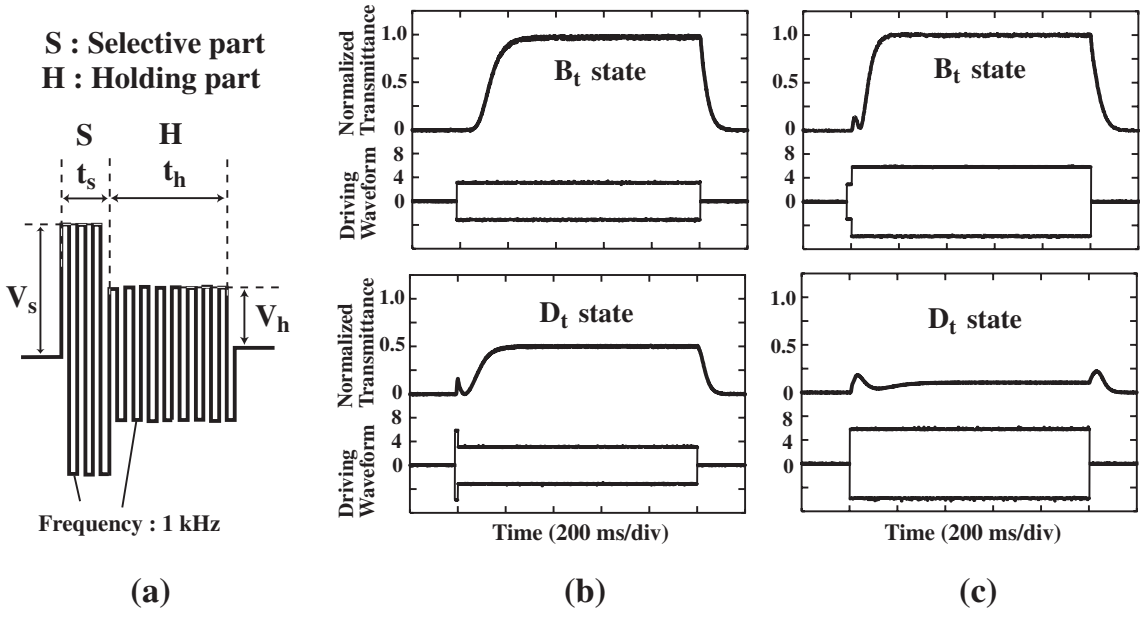

Fig. 3. (a) Schematic of the waveform for the switching bistability of the $\pi/2$-BCQH cell. (b) Switching bistability for $V_h = 3.2$ V. (c) Switching bistability for $V_h = 6$ V.

According to this concept, as illustrated in Fig. 3(a), we have designed a driving waveform which consists of two parts, namely, selective and holding parts. The selective part controls the flow effect of LCs and the holding part maintains the final state that we want. Figures 3(b) and 3(c) show the transient transmittance of the $\pi/2$-BCQH cell driven by two typical sets of new driving waveforms with different V_h values. The V_h in Fig. 3(b) is 3.2 V and that in Fig. 3(c) is 6 V. Figure 3(b) displays the switching bistability of the $\pi/2$-BCQH cell for low holding voltage between segments **ab** and **a′b′** in Fig. 2 obtained by changing the amplitude of the selective voltage, V_s, with the duration t_s of 10 ms. When $V_s = 3.2$ V, which is smaller than V_{sb}, a weak field-induced flow effect causes the switching of the $\mathbf{H}_t$ state to the $\mathbf{B}_t$ state. When $V_s = 6$ V, which is larger than V_{sb}, a strong flow effect induces the $\mathbf{H}_t$-to-$\mathbf{D}_t$ transition. Similarly, as illustrated in Fig. 3(c), the switching bistability for high holding voltage between segments **bc** and **b′c′** in Fig. 2 is also observed by changing the V_s with the duration t_s of 20 ms. For $V_s = 6\,\text{V} > V_{sb}$ and $V_s = 3.5\,\text{V} < V_{sb}$, one obtains the $\mathbf{D}_t$ and $\mathbf{B}_t$ states, respectively. Consequently, by applying the new driving waveforms, the switching bistability of the $\pi/2$-BCQH cell can be further expanded from the region $V_h \geq V_{sb}$ into an additional low-voltage region $V_{sb} > V_h \geq V_b$.

Relatively speaking, the $\mathbf{D}_t$ and $\mathbf{B}_t$ states can be achieved by strong and weak electrically induced flow effects, respectively. The key factors include not only the selective voltage V_s and holding voltage V_h, but also the duration t_s of the selective voltage for designing the bistable switching waveforms. For low holding voltage, i.e., $V_b < V_h < V_{sb}$, one can maintain V_s to be the same as V_h for the $\mathbf{B}_t$ state and adjust $V_s > V_{sb}$ and t_s for the $\mathbf{D}_t$ state. On the other hand, for a high holding voltage, i.e., $V_h > V_{sb}$, one can maintain V_s to be the same as V_h for the $\mathbf{D}_t$ state and adjust $V_s < V_{sb}$ and t_s to make the flow effect sufficiently weak for the $\mathbf{B}_t$ state. To illustrate this design rule, we measured the threshold time duration t_s^{th} for various selective voltages for each case.

Figure 4 displays the V_s-dependent time duration threshold t_s^{th} for different V_h value. The V_h in Fig. 4(a) is 3.5 V and that in Fig. 4(b) is 6 V. When $V_b < V_h < V_{sb}$, as shown in Fig. 4(a), the $\mathbf{H}_t$ to $\mathbf{D}_t$ transition can occur only when $t_s \geq t_s^{th}$. On the other hand, the $\mathbf{H}_t$-to-$\mathbf{B}_t$ transition can occur when $t_s < t_s^{th}$. In addition, we found that t_s^{th} decreases as V_s increases. It is reasonable to consider that the flow effect is proportional to the external field and that a stronger flow effect requires a shorter time in switching the cell to a larger twisted state, namely, the $\mathbf{D}_t$ state. Hence the increase in V_s results in the decrease in t_s^{th}. For $V_h > V_{sb}$, the results shown in Fig. 4(b) indicates two distinct features, compared with those shown in Fig. 4(a). First, the threshold t_s values for the $\mathbf{H}_t$-to-$\mathbf{B}_t$ transition and the $\mathbf{H}_t$-to-$\mathbf{D}_t$ transition are different. We designated $t_s^{th}(\mathbf{B}_t)$ for the $\mathbf{H}_t$-to-$\mathbf{B}_t$ transition and $t_s^{th}(\mathbf{D}_t)$ for the $\mathbf{H}_t$-to-$\mathbf{D}_t$ transition. Second, $t_s^{th}(\mathbf{B}_t)$ and $t_s^{th}(\mathbf{D}_t)$ are the minimum and maximum time durations for the $\mathbf{H}_t$-to-$\mathbf{B}_t$ transition and the $\mathbf{H}_t$-to-$\mathbf{D}_t$ transition with single domain, respectively, for high V_h. This is opposite to those observed in Fig. 4(a) for low V_h. In addition, in the region $t_s^{th}(\mathbf{B}_t) > t_s > t_s^{th}(\mathbf{D}_t)$, the $\mathbf{H}_t$ state transits to both $\mathbf{B}_t$ and $\mathbf{D}_t$, resulting in the formation of a polydomain. However, outside this region, the uniform $\mathbf{B}_t$ or $\mathbf{D}_t$ state is observed. Furthermore, we found that t_s^{th} also depends on the material's elastic constant, d/p ratio and boundary conditions. A detailed investigation is in progress.

In summary, we demonstrated an electrically switching $\pi/2$-BCQH device with low driving voltage. This device operates from the initial twisted-homeotropic state into either $+90°$ or $-270°$ twisted state by controlling the slew rate of the driving square pulses. The critical voltage for the switching bistability is only 4.3 V, which is about twice its V_{th}. However, we found that the bistable property of this device also exists in a bias voltage between 3 and 4.3 V, but the field-induced flow effect in this region was insufficient strong to achieve the switching bistability by only controlling the slew rate of the driving square pulses. We proposed a modified driving waveform, which is composed of the

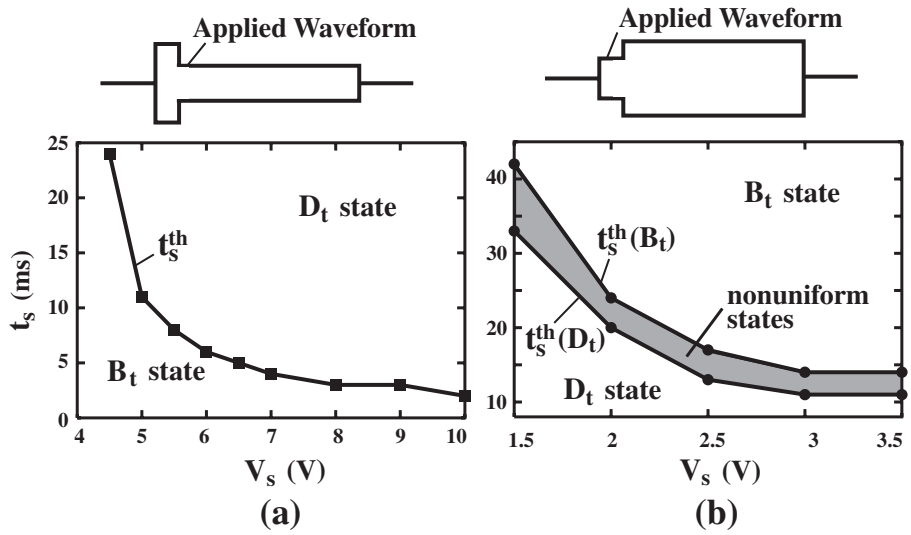

Fig. 4. Thresholds of the time duration for the selective part, t_s^{th}, as a function of the selective voltage V_s with different holding voltage V_h values. (a) $V_h = 3.5$ V. (b) $V_h = 6$ V.

selective and holding parts, for switching this device. The selective part controls the flow effect of LCs and the holding part maintains the final state that we want. Consequently, the switching bistability was further expanded into the region between 3 and 4.3 V by controlling the amplitude and duration of the selective part. The threshold time duration of the selective part was also examined and presented in the phase diagrams.

This work was partially supported by the National Science Council, R.O.C., under Contract No. NSC-91-2112-M-009-025. The ITO glass support of Chi-Mei Opto. Co. is greatly appreciated.

1) D. W. Berreman and W. R. Heffner: J. Appl. Phys. **52** (1981) 3032.
2) T. Z. Qian, Z. L. Xie, H. S. Kwok and P. Sheng: Appl. Phys. Lett. **71** (1997) 596.
3) H. Bock: Appl. Phys. Lett. **73** (1998) 2905.
4) Z. L. Xie and H. S. Kwok: J. Appl. Phys. **84** (1998) 77.
5) B. Wang and P. J. Bos: J. Appl. Phys. **90** (2001) 552.
6) I. Dozov, M. Nobili and G. Durand: Appl. Phys. Lett. **70** (1997) 1179.
7) R. Barberi, M. Giocondo, J. Li, R. Bartolino, I. Dozov and G. Durand: Appl. Phys. Lett. **71** (1997) 3495.
8) J. X. Guo and H. S. Kwok: Appl. Phys. Lett. **77** (2000) 3716.
9) Z. L. Xie, Z. G. Meng, M. Wong and H. S. Kwok: Appl. Phys. Lett. **81** (2002) 2553.
10) G. P. Bryan-Brown, M. J. Towler, M. S. Bancroft and D. G. McDonnell: *Proc. Int. Disp. Res. Conf. 1994* (SID, Santa Ana, 1994) p. 209.
11) L. Y. Chen and S. H. Chen: Appl. Phys. Lett. **74** (1999) 3779.
12) C. Y. Hsieh and S. H. Chen: Appl. Phys. Lett. **83** (2003) 1110.
13) S. W. Shu, S. T. Shin and S. D. Lee: Appl. Phys. Lett. **68** (1996) 2819.
14) S. T. Wu, C. S. Wu and K. W. Lin: J. Appl. Phys. **82** (1997) 4795.
15) S. H. Chen and L. Y. Chen: Appl. Phys. Lett. **75** (1999) 3491.